Eur. Phys. J. B **54**, 113–119 (2006)
DOI: 10.1140/epjb/e2006-00418-0

THE EUROPEAN PHYSICAL JOURNAL B

1D stability analysis of filtering and controlling the solitons in Bose-Einstein condensates

S. De Nicola[1], R. Fedele[2,a], D. Jovanovic[3], B. Malomed[4], M.A. Man'ko[5], V.I. Man'ko[5], and P.K. Shukla[6]

[1] Istituto di Cibernetica "Eduardo Caianiello" del CNR Comprensorio "A. Olivetti" Fabbr. 70, Via Campi Flegrei, 34, 80078 Pozzuoli (NA), Italy
[2] Dipartimento di Scienze Fisiche, Università Federico II and INFN Sezione di Napoli, Complesso Universitario di M.S. Angelo, via Cintia, 80126 Napoli, Italy
[3] Institute of Physics, P.O. Box 57, 11001 Belgrade, Serbia
[4] Department of Interdisciplinary Studies, School of Electrical Engineering, Faculty of Engineering, Tel Aviv University, Tel Aviv 69978, Israel
[5] P.N. Lebedev Physical Institute, Leninskii Prospect 53, Moscow 119991, Russia
[6] Institut für Theoretische Physik IV and Centre for Plasma Science and Astrophysics, Fakultät für Physik und Astronomie, Ruhr–Universität Bochum, 44780 Bochum, Germany

Received 28 August 2006
Published online 24 November 2006 –

Abstract. We present one-dimensional (1D) stability analysis of a recently proposed method to filter and control localized states of the Bose–Einstein condensate (BEC), based on novel trapping techniques that allow one to conceive methods to select a particular BEC shape by controlling and manipulating the external potential well in the three-dimensional (3D) Gross–Pitaevskii equation (GPE). Within the framework of this method, under suitable conditions, the GPE can be exactly decomposed into a pair of coupled equations: a transverse two-dimensional (2D) linear Schrödinger equation and a one-dimensional (1D) longitudinal nonlinear Schrödinger equation (NLSE) with, in a general case, a time-dependent nonlinear coupling coefficient. We review the general idea how to filter and control localized solutions of the GPE. Then, the 1D longitudinal NLSE is numerically solved with suitable non-ideal controlling potentials that differ from the ideal one so as to introduce relatively small errors in the designed spatial profile. It is shown that a BEC with an asymmetric initial position in the confining potential exhibits breather-like oscillations in the longitudinal direction but, nevertheless, the BEC state remains confined within the potential well for a long time. In particular, while the condensate remains essentially stable, preserving its longitudinal soliton-like shape, only a small part is lost into "radiation".

PACS. 03.75.Lm Tunneling, Josephson effect, Bose-Einstein condensates in periodic potentials, solitons, vortices, and topological excitations – 05.45.Yv Solitons – 05.30.Jp Boson systems – 03.65.Ge Solutions of wave equations: bound states

1 Introduction

The main feature of a system of identical quantum particles is that the particles are truly indistinguishable [1]. Due to this property, a system of quantum particles follows a statistics which differs substantially from the classical one [2]. The equilibrium distribution of bosons obeys the well-known Bose–Einstein distribution which differs from the Mawxell–Boltzmann distribution and predicts degenerate states. The effects of deviation from the classical mechanics appear when the thermal de Broglie wavelength exceeds the mean inter-particle distance (i.e., when the overlapping of the single–particle wavefunctions takes place). In particular, in a gas of identical bosons the particles may stimulate each other to occupy the lowest energy state leading to a sort of phase transition called Bose–Einstein condensation (BEC) [3,4]. The product of this process is a macroscopic quantum-mechanical object which can be described by a macroscopic quantum wavefunction. In the recent years, a number of important theoretical and experimental investigations on the physics and possible technological applications of BEC have been done [5–7]. In particular, a BEC state of ^{87}Rb atoms has been experimentally achieved for the first time in 1995 [8], soon followed by similar experiments with ^{23}Na [9] and ^{7}Li [10] atoms. The experimental realization of BEC states is of a fundamental importance to verify the prediction of the Bose–Einstein theory. In fact, except for ^{4}He, which is a superfluid at very low temperature, under the physical conditions required for the thermodynamical equilibrium

[a] e-mail: renato.fedele@na.infn.it

of the atomic condensate, all other materials are in the solid state.

It is well known that the Bose–Einstein condensate has to be created in suitable trapping devices. In fact, the experimental demonstration of BECs was possible thanks to the very advanced trapping techniques that use laser cooling (very efficient for alkali atoms) in combination with magnetic confinement and evaporative cooling (developed for hydrogen) [11,12]. Very recently developed techniques involving lithographically fabricated circuit patterns, which provide electromagnetic guides and microtraps for ultracold neutral systems of atoms in BEC experiments [13], have the possibility to produce almost arbitrary space profiles of the trapping potential. Alternatively, the use of optically induced potentials is also extremely versatile for the production of "exotic" potentials [14]. Thus, the present technology allows one to design almost arbitrary potential wells that are needed to reach a particular goal in a BEC experiment. This possibility allows one, in turn, to conceive methods to select desired BEC spatial profiles by manipulating and controlling the trapping potential well. As shown recently in a theoretical investigation [15], this kind of filtering and controlling operation reduces to a few external physical parameters. This method has been actually employed to filter and control stationary soliton-like states associated to the longitudinal BEC dynamics.

The three-dimensional (3D) dynamics of BECs in a spatially nonuniform confining potential well is governed by the 3D Gross–Pitaevskii equation (GPE) [16], viz.,

$$i\hbar\frac{\partial\Psi(\mathbf{r},t)}{\partial t} = -\frac{\hbar^2}{2m_a}\nabla^2\Psi(\mathbf{r},t) + U\left[\mathbf{r},t,|\Psi(\mathbf{r},t)|^2\right]\Psi, \quad (1)$$

where $\hbar$ is the Planck's constant divided by 2π, $\Psi(\mathbf{r},t)$ is the macroscopic wavefunction of the condensate, m_a is the atomic mass, the functional $U\left[\mathbf{r},t,|\Psi(\mathbf{r},t)|^2\right] = V_{\rm ext}(\mathbf{r},t) + gN|\Psi(\mathbf{r},t)|^2$ is the total potential energy, $V_{\rm ext}(\mathbf{r},t)$ is the external confining potential for BECs, the coupling constant g is related to the short range scattering (s-wave) length a representing the interactions between atomic particles, namely, $g = 4\pi\hbar^2 a/m_a$, and N is the number of atoms. The short range scattering length a of atoms can be either positive or negative giving rise to either attractive or repulsive forces.

Stationary solutions of equation (1) in one space dimension can be cast in the form of solitons [17]. The formation of bright and dark/grey solitons, observed experimentally in elongated BECs [18], is attributed to the attractive as well as repulsive inter-atomic interaction.

Recently, a method to obtain exact localized controlled solutions of the three-dimensional 3D GPE (1) for ground and excited states has been proposed [15]. When suitable external controlling potentials are imposed, the GPE can be exactly decomposed in a linear two-dimensional (2D) Schrödinger equation (transverse equation) and a one-dimensional (1D) nonlinear Schrödinger equation (longitudinal equation).

In this paper, we present a 1D stability analysis of the controlled BEC solutions obtained in reference [15]. We perturb around the ideal controlling potential that makes possible the exact controlled solution. Then, a 1D stability analysis is performed numerically.

In Section 2, we briefly review the general idea how to filter and control localized solutions whose dynamics is governed by the 3D GPE. This idea is applied to BEC to control longitudinal localized profiles. The time-dependent wavefunction of the total macroscopic BEC state is factorized in the product of two time-dependent wavefunctions depending on the longitudinal coordinate, say z (along which the soliton-like shape has to be created), and the transverse coordinates, say x and y, respectively. Correspondingly, the 3D GPE is exactly decomposed into a pair of coupled equations: a 2D linear Schrödinger equation (LSE) defined on the transverse configurational $x-y$ plane, plus a 1D nonlinear Schrödinger equation (NLSE) defined on the configurational z axis. In Section 3, explicit exact analytical controlled localized 3D solutions of the BEC, consisting in transverse 2D Hermite-Gauss modes plus a longitudinal bright soliton, are found and numerically evaluated. In Section 4, the stability of the controlling potential method is numerically tested, confining our attention to the 1D longitudinal equation. Finally, in Section 5 some remarks and the conclusions are presented.

2 The basic idea of filtering and controlling localized solutions of the 3D GPE

First, we note that under the common experimental conditions in which the external potential is composed of two parts, viz., $V_{\rm ext}(\mathbf{r},t) = V_\perp(\mathbf{r}_\perp,t) + V_z(\mathbf{r}_\perp,z,t)$, there exists a solution of equation (1) that separates the spatial variables, provided the potential $V_z(\mathbf{r}_\perp,z,t)$ is appropriately tuned. To show this, first we look for the solution of equation (1) in the form $\Psi(\mathbf{r},z,t) = \Psi_\perp(\mathbf{r}_\perp,t)\Psi_z(\mathbf{r}_\perp,z,t)$, which permits us to rewrite the GP equation (1) as

$$\Psi_\perp\left[i\hbar\frac{\partial\Psi_z}{\partial t} + \frac{\hbar^2}{2m_a}\left(\frac{\partial^2}{\partial z^2} + \nabla_\perp^2 + \frac{2}{\Psi_\perp}\nabla_\perp\Psi_\perp\cdot\nabla_\perp\right)\Psi_z - gN|\Psi_\perp|^2|\Psi_z|^2\Psi_z - V_z(\mathbf{r}_\perp,z,t)\Psi_z\right] = -\Psi_z\left[i\hbar\frac{\partial\Psi_\perp}{\partial t} + \frac{\hbar^2}{2m_a}\nabla_\perp^2\Psi_\perp - V_\perp(\mathbf{r}_\perp,t)\Psi_\perp\right]. \quad (2)$$

The function $\Psi_\perp$ is adopted so that it satisfies the following 2D linear Schrödinger equation:

$$i\hbar\frac{\partial\Psi_\perp}{\partial t} + \frac{\hbar^2}{2m_a}\nabla_\perp^2\Psi_\perp - V_\perp(\mathbf{r}_\perp,t)\Psi_\perp = 0\,, \quad (3)$$

and consequently, the right-hand-side of equation (2) reduces to zero.

Next, we note that there exists a particular form of the potential $V_z(\mathbf{r}_\perp,z,t)$ that admits purely one dimensional solutions Ψ_z (independent of $\mathbf{r}_\perp$). An obvious choice for such potential is

$$V_z(\mathbf{r}_\perp,z,t) = V(z,t) + g_{1D}(t)N|\Psi_z|^2 - gN|\Psi_\perp|^2|\Psi_z|^2, \quad (4)$$

where $V(z,t)$ and $g_{1D}(t)$ are arbitrary functions of their arguments. However, the potential (4) is expressed via the solution for Ψ_z that is still unknown, and to proceed we need to solve the GPE (2). The latter, after the substitution of equation (4), yields:

$$i\hbar\frac{\partial\Psi_z}{\partial t} = -\frac{\hbar^2}{2m_a}\left(\frac{\partial^2}{\partial z^2} + \nabla_\perp^2 + \frac{2}{\Psi_\perp}\nabla_\perp\Psi_\perp\cdot\nabla_\perp\right)\Psi_z + g_{1D}(t)N|\Psi_z|^2\Psi_z + V(z,t)\Psi_z\,, \quad (5)$$

which is considerably easier to solve than the original 3D GPE. Its coefficients depend only on z and t, and consequently it possesses purely 1D solutions with $\nabla_\perp\Psi_z = \nabla_\perp^2\Psi_z = 0$.

One simple choice for the coefficients $V(z,t)$ and $g_{1D}(t)$ is found if we multiply equation (5) by $|\Psi_\perp|^2$ and integrate over the entire transverse plane, assuming a purely 1D function Ψ_z and the function $\Psi_\perp$ that satisfies equation (3). We also assume the usual normalization conditions for $\Psi_\perp$ and Ψ_z (and consequently for the total wave function Ψ),

$$\int |\Psi_\perp|^2\, d^2r_\perp = \int |\Psi_z|^2\, dz = 1. \quad (6)$$

Such procedure readily yields the following 1D GPE

$$i\hbar\frac{\partial\Psi_z}{\partial t} = -\frac{\hbar^2}{2m_a}\frac{\partial^2\Psi_z}{\partial z^2} + g_{1D}(t)N|\Psi_z|^2\Psi_z + V(z,t)\Psi_z\,, \quad (7)$$

with

$$g_{1D}(t) = g\int |\Psi_\perp(\mathbf{r}_\perp,t)|^4 d^2r_\perp \quad (8)$$

and

$$V(z,t) = \int V_z(\mathbf{r}_\perp,z,t)|\Psi_\perp(\mathbf{r}_\perp,t)|^2\, d^2r_\perp. \quad (9)$$

In conclusion, equation (5) provides an exact 1D equation for Ψ_z, described by equation (7). This is equivalent to saying that equation (5) has 1D solutions $\Psi_z = \Psi_z(z,t)$ in such a way that equation (2) admits solutions in the factorized form $\Psi(\mathbf{r},z,t) = \Psi_\perp(\mathbf{r}_\perp,t)\Psi_z(z,t)$. Equation (7) is coupled to equation (3) through the nonlinear coupling coefficient $g_{1D}(t)$ which depends on the shape of $\Psi_\perp$ and may be thought of as a functional of $\Psi_\perp$. Additionally, g_{1D} depends on time which makes the longitudinal dynamics of BEC non stationary. Within this framework, to reach experimentally stationary longitudinal configurations, some controlling operations for g_{1D} are necessary.

Filtering and controlling a solution of equation (5) implies an "a priori" choice of the desired solution, say $\tilde{\Psi}_z$. The latter is adopted within a given family of possible solutions (e.g. single-soliton solutions, multi-soliton solutions, periodic solutions, etc.) obeying given initial conditions. Subsequently, this choice allows us to find the external potential, say $\tilde{V}(z,t)$, that self-consistently determines the solution with such particular initial condition. The operation of finding the appropriate potential well implies that V, defined by equation (9), can be thought of as a functional of Ψ_z, viz., $V[\Psi_z]$. Thus, we first find the explicit form of such a functional. In turn, we find the explicit form of $\tilde{V}$ as a function of z and t, for a given solution $\tilde{\Psi}_z$, i.e., $\tilde{V}(z,t) = V[\tilde{\Psi}_z(z,t)]$.

In particular, we want to select from (7) a stationary bright soliton with the given amplitude A_M and length l_z. Consequently, our desired solution is

$$\tilde{\Psi}_z = A_M\ \mathrm{sech}\,(z/l_z)\exp\left(-iEt/\hbar\right)\,, \quad (10)$$

which obeys the initial condition: $\tilde{\Psi}_z(z,0) = A_M\ \mathrm{sech}\,(z/l_z)$. We note that the function (10) is the solution of the following cubic NLSE

$$i\hbar\partial\tilde{\Psi}_z/\partial t = -(\hbar^2/2m_a)\partial^2\tilde{\Psi}_z/\partial z^2 + \beta|\tilde{\Psi}_z|^2\tilde{\Psi}_z\,, \quad (11)$$

where $\beta = -\hbar^2/m_a l_z^2 A_M^2 < 0$ and $E = -\hbar^2/2m_a l_z^2 < 0$. In particular, if $\tilde{\Psi}_z$ is normalized, it follows that $A_M = 1/\sqrt{2l_z}$ and $\beta = -2\hbar/m_a l_z$.

In order to find the form of the functional $V[\Psi_z]$, we note that equations (7) and (11) admit by construction the same solution that we want to select. Thus, by assuming that $\Psi_z = \tilde{\Psi}_z$, and combining equations (7) and (11), we easily get the following condition of consistency which defines the functional $V[\Psi_z]$, viz.,

$$V[\Psi_z] = \left[\beta - g_{1D}(t)N\right]|\Psi_z|^2\,. \quad (12)$$

Correspondingly, the explicit dependence in space and time of $\tilde{V}$ is given by:

$$\tilde{V}(z,t) = -\left(\hbar^2/m_a l_z^2\right)\left[1 + \left(m_a N l_z/2\hbar^2\right)\, g_{1D}(t)\right]\ \mathrm{sech}^2\,(z/l_z)\,. \quad (13)$$

Note that the external longitudinal potential well is time-modulated through the factor $g_{1D}(t)$.

It should be noted that just the filtering of our solution is not sufficient. To ensure its long life, the selected solution needs to be controlled. This can be done by tuning the shape of the potential well given by equation (13), i.e., by adjusting few external physical parameters that allow us to produce this shape, in view of using the techniques described in [13,14]), as well as the function $g_{1D}(t)$ which, in turn, is given by monitoring and controlling the transverse BEC dynamics (note that the sign of g_{1D} depends on the sign of the scattering length).

3 Controlled localized BEC solutions in a transverse harmonic potential well

In this section, we analyze the role of the transverse BEC dynamics played in controlling the longitudinal dynamics through the time-dependent parameter $g_{1D}(t)$. As equation (3) is linear, its arbitrary solution can be expressed as the linear combination of the corresponding linear eigenfunctions. It is convenient to use a time-dependent complete set of eigenfunctions, which permits us to determine

the time-dependent parameter $g_{1D}(t)$ in a straightforward manner.

The transverse external potential that is involved in BEC experiments is usually parabolic, i.e., $V_\perp(x,y,t) \equiv m_a\left[\omega_x^2(t)x^2+\omega_y^2(t)y^2\right]/2$. Then, in Cartesian coordinates, equation (3) admits the following complete set of normalized Hermite–Gauss modes:

$$\Psi_{\perp nm}(x,y,t) \;=\; \Psi_{xn}(x,t)\Psi_{ym}(y,t)\,, \qquad (14)$$

where

$$\Psi_{jk}(j,t) = H_k\left[j/\sqrt{2}\sigma_j(t)\right] \times \frac{\exp\left[-j^2/4\sigma_j^2(t)+im_a\gamma_j(t)j^2/2\hbar+i\phi_{jk}(t)\right]}{\left[2\pi\sigma_j^2(t)2^{2k}(k!)^2\right]^{1/4}}, \qquad (15)$$

with $j=x,y$ and $k=0,1,2,3,...$ The quantities $\sigma_j(t)$, $\gamma_j(t)$ and ϕ_{jk} satisfy the following system of equations

$$d^2\sigma_j/dt^2+\omega_j^2(t)\sigma_j-\hbar^2/4m_a^2\sigma_j^3=0, \qquad (16)$$

$\gamma_j(t)=(1/\sigma_j(t))(d\sigma_j(t)/dt)$, $\phi_{jk}(t)=(2k+1)\,\phi_{j0}(t)$, and $d\phi_{j0}(t)/dt=-\hbar/4m_a\sigma_j^2(t)$. By virtue of the linearity of equation (3), an arbitrary normalized solution $\Psi_\perp$ can be expressed as a linear combination of the above $\Psi_{\perp nm}$, i.e. $\Psi_\perp=\Sigma_{nm}c_{nm}\Psi_{\perp nm}$. Note that $\Psi_{j0}(j,t)$ is a purely Gaussian time-dependent fundamental mode associated with the jth transverse direction and $\sigma_j(t)$ is its rms $\sqrt{\langle j^2\rangle}$. Consequently, the transverse effective spot size of the condensate can be defined as $\sigma_\perp(t)\equiv\sqrt{\sigma_x^2(t)+\sigma_y^2(t)}$. The Pinney equation (16) describes the envelope oscillations of the condensate along the jth transverse direction within the quadratic potential well $V_j(j,t)=m_a\omega_j^2(t)j^2/2$. Note the full similarity between equation (16) and the one describing the envelope dynamics of a charged-particle beam in an accelerating machine [19] through a quadrupole-like or the envelope dynamics of an electromagnetic radiation beam in an optical medium [20] through a linear optical lens, respectively. In these cases, $\hbar$ is replaced by the transverse beam emittance or by the radiation wavelength, respectively.

For the sake of simplicity, we assume that the ω_j are independent of time, then equation (16) can be easily integrated. For the initial conditions $\sigma_{j0}\equiv\sigma_j(t=0)$ and $\gamma_{j0}\equiv\gamma_j(t=0)$, the BEC transverse envelope motion is described by

$$\sigma_j(t)=\sigma_{j0}\left[\left(\cos\omega_j t+\frac{\gamma_{j0}}{\omega_j}\sin\omega_j t\right)^2+\frac{\sigma_j^{*4}}{\sigma_{j0}^4}\sin^2\omega_j t\right]^{1/2}, \qquad (17)$$

where $\sigma_j^*=\sqrt{\hbar/2m_a\omega_j}$. From equation (17) it is evident that, if $\gamma_{j0}\neq 0$, BECs execute envelope oscillations (breathings). Conversely, when $\gamma_{j0}=0$, the jth transverse BEC state is described by a wavefunction [given for each integer k by equation (15)] whose rms does not change in time (stationary state) when $\sigma_{j0}=\sigma_j^*$ (matched case), or it executes oscillations when $\sigma_{j0}\neq\sigma_j^*$ (unmatched case). In particular, for $k=0$, the transverse state along x and the one along y are described by the 1D harmonic oscillator ground state, respectively.

Assuming that, by virtue of equation (15), $\Psi_\perp=\Psi_{\perp nm}$ we have

$$g_{1D}^{(nm)}(t)\equiv g\int|\Psi_{\perp nm}(x,y,t)|^4d^2r_\perp\,, \qquad (18)$$

which can be rewritten as

$$g_{1D}^{(nm)}(t)=g\;\delta_n\delta_m/2\pi^2\sigma_x(t)\sigma_y(t)\,, \qquad (19)$$

where

$$\delta_k=\frac{1}{2^{2k}(k!)^2}\int_{-\infty}^{\infty}\exp\left(-2\xi^2\right)\left[H_k(\xi)\right]^4d\xi. \qquad (20)$$

Let us now discuss how the time dependence of g_{1D} explicitly affects the control operations when the factorized solutions (14) is assumed. Having a solution $\Psi_{\perp nm}(x,y,t)$, one has control tools for the longitudinal soliton solution of the GPE. These tools are reduced to time-dependent variable $g_{1D}(t)$. Even if each ω_j is independent of time, each $\sigma_j(t)$ is given by equation (17) and therefore depends on time. Consequently, the external potential well (13) assumes the form:

$$V(z,t)=-\frac{\hbar^2}{m_a l_z^2}\left[1+\frac{m_aNl_zg\delta_n\delta_m}{4\pi^2\hbar^2\sigma_x(t)\sigma_y(t)}\right]\mathrm{sech}^2\left(z/l_z\right). \qquad (21)$$

Taking into account solutions (14), it is easy to see that the transverse BEC probability density of matter waves $|\Psi_{\perp nm}(x,y,t)|^2$ is affected by oscillatory breathers. This means that the operations of filtering and controlling a stationary bright soliton of given width must take into account this effect of transverse BEC "respiration". It turns out that, in order to filter and control a longitudinal bright soliton profile of BEC while preserving its width, one has to impose an external potential well given by (21), which takes into account the transverse BEC breathers. In general, due to the linearity of equation (3), an arbitrary transverse BEC state $\Psi_\perp$, which can be expressed as a superposition of the Hilbert space base $\{\Psi_{\perp nm}\}$, should exhibit similar oscillatory behavior as well. Figures 1–7 clearly show the oscillations of both the BEC transverse density distributions due to the transverse rms (spot size) oscillations. While this BEC "respiration" takes place, the soliton-like BEC longitudinal profile remains unchanged. For $n=m=0$, the 2D transverse BEC cross-section (transverse spot) is an ellipse whose shape changes periodically as the ratio $\sigma_x(t)/\sigma_y(t)$ changes in time. In particular, this ratio, which initially is <1, reaches 1, and subsequently becomes >1. For n and/or m greater than 1, there is more than one transverse spot. For increasing values of n and m (higher modes), the numbers of transverse spots increase correspondingly and the time evolution of all the transverse spots shows the oscillatory behavior.

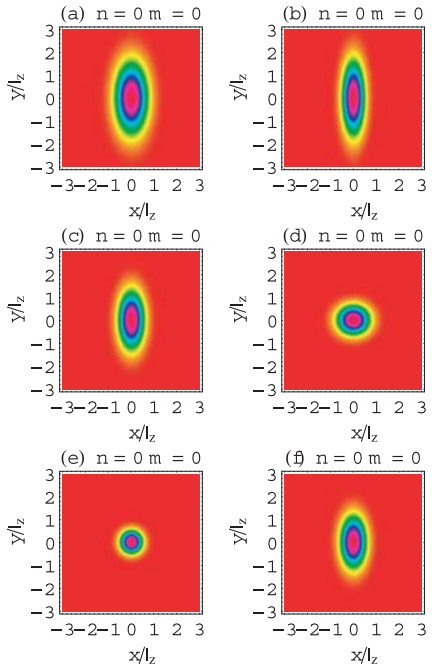

Fig. 1. Cross sections of the BEC transverse probability density $|\Psi_{\perp 00}|^2$ at $z = 0$ and different times : $t_1 = 3.14/3\omega_x$ (a), $t_2 = 6.28/3\omega_x$ (b), $t_3 = 3.14/\omega_x$ (c), and $t_4 = 12.56/3\omega_x$ (d), $t_5 = 15.70/3\omega_x$ (e), $t_6 = 6.28/\omega_x$ (f). Calculations refer to $\omega \equiv \omega_y/\omega_x = 0.5$, $\sigma_x^*/l_z = 0.5$, $\sigma_y^*/l_z = \sigma_x^*/l_z\sqrt{\omega} = 1/\sqrt{2}$. Normalized transverse widths are $\sigma_{x0}/l_z = 0.5$ and $\sigma_{y0}/l_z = 1$; $\gamma_{x0}/\omega_x = 0.5$ and $\gamma_{y0}/\omega_y = 1$.

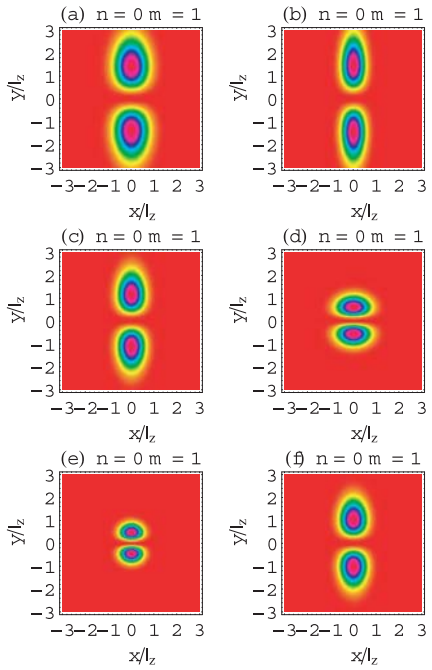

Fig. 2. Cross sections of the BEC transverse probability density $|\Psi_{\perp 01}|^2$ at $z = 0$ and different times : $t_1 = 3.14/3\omega_x$ (a), $t_2 = 6.28/3\omega_x$ (b), $t_3 = 3.14/\omega_x$ (c), and $t_4 = 12.56/3\omega_x$ (d), $t_5 = 15.70/3\omega_x$ (e), $t_6 = 6.28/\omega_x$ (f). Calculations refer to $\omega \equiv \omega_y/\omega_x = 0.5$, $\sigma_x^*/l_z = 0.5$, $\sigma_y^*/l_z = \sigma_x^*/l_z\sqrt{\omega} = 1/\sqrt{2}$. Normalized transverse widths are $\sigma_{x0}/l_z = 0.5$ and $\sigma_{y0}/l_z = 1$; $\gamma_{x0}/\omega_x = 0.5$ and $\gamma_{y0}/\omega_y = 1$.

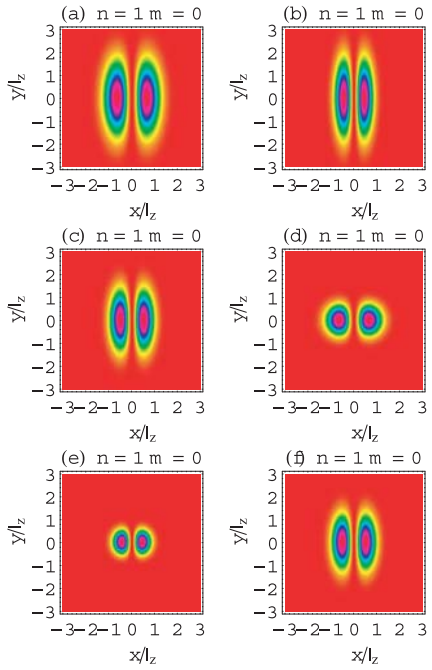

Fig. 3. Cross sections of the BEC transverse probability density $|\Psi_{\perp 10}|^2$ at $z = 0$ and different times : $t_1 = 3.14/3\omega_x$ (a), $t_2 = 6.28/3\omega_x$ (b), $t_3 = 3.14/\omega_x$ (c), and $t_4 = 12.56/3\omega_x$ (d), $t_5 = 15.70/3\omega_x$ (e), $t_6 = 6.28/\omega_x$ (f). Calculations refer to $\omega \equiv \omega_y/\omega_x = 0.5$, $\sigma_x^*/l_z = 0.5$, $\sigma_y^*/l_z = \sigma_x^*/l_z\sqrt{\omega} = 1/\sqrt{2}$. Normalized transverse widths are $\sigma_{x0}/l_z = 0.5$ and $\sigma_{y0}/l_z = 1$; $\gamma_{x0}/\omega_x = 0.5$ and $\gamma_{y0}/\omega_y = 1$.

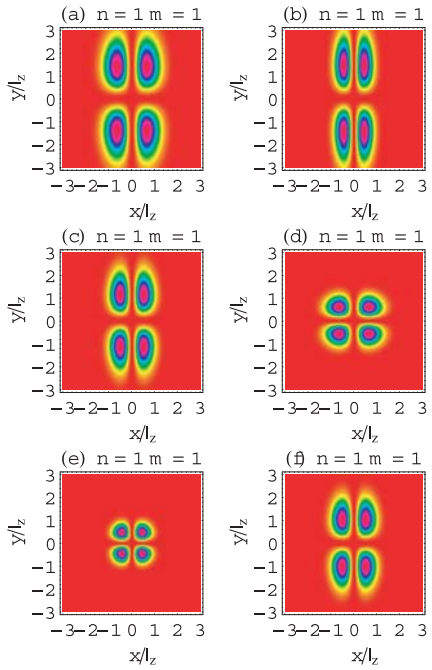

Fig. 4. Cross sections of the BEC transverse probability density $|\Psi_{\perp 11}|^2$ at $z = 0$ and different times : $t_1 = 3.14/3\omega_x$ (a), $t_2 = 6.28/3\omega_x$ (b), $t_3 = 3.14/\omega_x$ (c), and $t_4 = 12.56/3\omega_x$ (d), $t_5 = 15.70/3\omega_x$ (e), $t_6 = 6.28/\omega_x$ (f). Calculations refer to $\omega \equiv \omega_y/\omega_x = 0.5$, $\sigma_x^*/l_z = 0.5$, $\sigma_y^*/l_z = \sigma_x^*/l_z\sqrt{\omega} = 1/\sqrt{2}$. Normalized transverse widths are $\sigma_{x0}/l_z = 0.5$ and $\sigma_{y0}/l_z = 1$; $\gamma_{x0}/\omega_x = 0.5$ and $\gamma_{y0}/\omega_y = 1$.

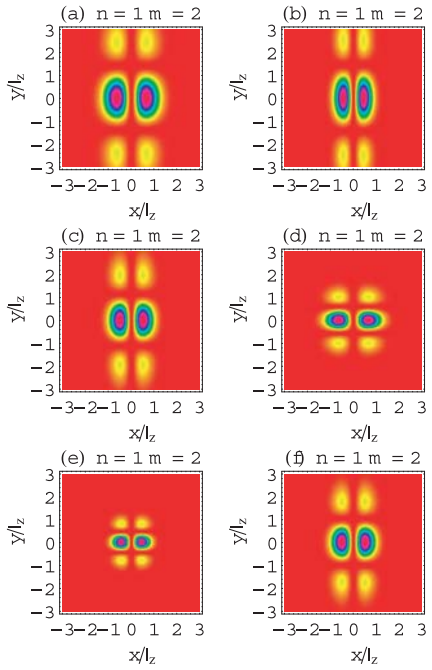

Fig. 5. Cross sections of the BEC transverse probability density $|\Psi_{\perp 12}|^2$ at $z = 0$ and different times : $t_1 = 3.14/3\omega_x$ (a), $t_2 = 6.28/3\omega_x$ (b), $t_3 = 3.14/\omega_x$ (c), and $t_4 = 12.56/3\omega_x$ (d), $t_5 = 15.70/3\omega_x$ (e), $t_6 = 6.28/\omega_x$ (f). Calculations refer to $\omega \equiv \omega_y/\omega_x = 0.5$, $\sigma_x^*/l_z = 0.5$, $\sigma_y^*/l_z = \sigma_x^*/l_z\sqrt{\omega} = 1/\sqrt{2}$. Normalized transverse widths are $\sigma_{x0}/l_z = 0.5$ and $\sigma_{y0}/l_z = 1$; $\gamma_{x0}/\omega_x = 0.5$ and $\gamma_{y0}/\omega_y = 1$.

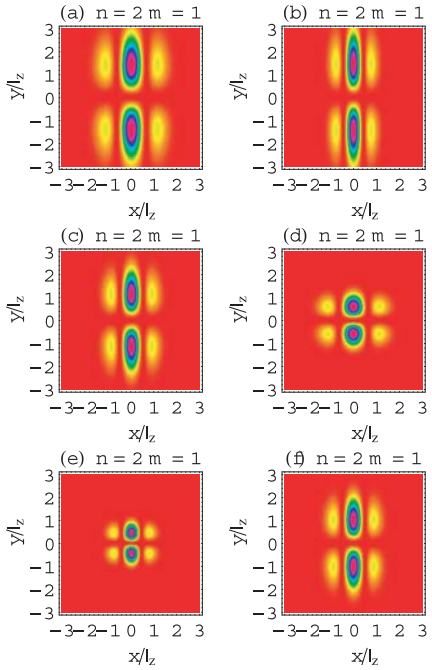

Fig. 6. Cross sections of the BEC transverse probability density $|\Psi_{\perp 21}|^2$ at $z = 0$ and different times : $t_1 = 3.14/3\omega_x$ (a), $t_2 = 6.28/3\omega_x$ (b), $t_3 = 3.14/\omega_x$ (c), and $t_4 = 12.56/3\omega_x$ (d), $t_5 = 15.70/3\omega_x$ (e), $t_6 = 6.28/\omega_x$ (f). Calculations refer to $\omega \equiv \omega_y/\omega_x = 0.5$, $\sigma_x^*/l_z = 0.5$, $\sigma_y^*/l_z = \sigma_x^*/l_z\sqrt{\omega} = 1/\sqrt{2}$. Normalized transverse widths are $\sigma_{x0}/l_z = 0.5$ and $\sigma_{y0}/l_z = 1$; $\gamma_{x0}/\omega_x = 0.5$ and $\gamma_{y0}/\omega_y = 1$.

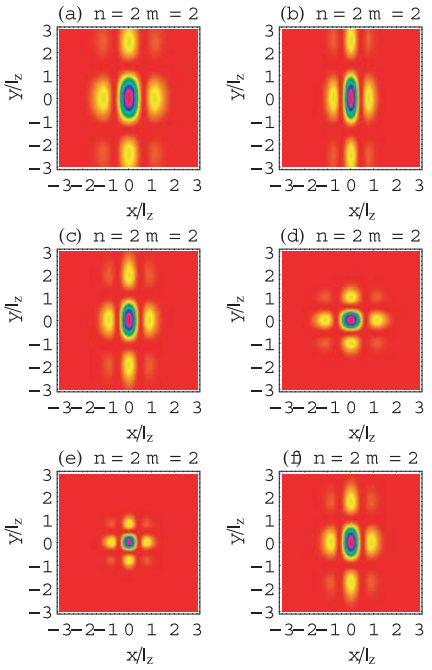

Fig. 7. Cross sections of the BEC transverse probability density $|\Psi_{\perp 22}|^2$ at $z = 0$ and different times : $t_1 = 3.14/3\omega_x$ (a), $t_2 = 6.28/3\omega_x$ (b), $t_3 = 3.14/\omega_x$ (c), and $t_4 = 12.56/3\omega_x$ (d), $t_5 = 15.70/3\omega_x$ (e), $t_6 = 6.28/\omega_x$ (f). Calculations refer to $\omega \equiv \omega_y/\omega_x = 0.5$, $\sigma_x^*/l_z = 0.5$, $\sigma_y^*/l_z = \sigma_x^*/l_z\sqrt{\omega} = 1/\sqrt{2}$. Normalized transverse widths are $\sigma_{x0}/l_z = 0.5$ and $\sigma_{y0}/l_z = 1$; $\gamma_{x0}/\omega_x = 0.5$ and $\gamma_{y0}/\omega_y = 1$.

4 1D stability analysis of BEC control procedures

Under realistic experimental conditions, one may expect that the controlling potential V is realized with a certain error relative to its desired form, given by equation (13). It is necessary to investigate the dynamics of BECs in such nonideal traps and, in particular, to check whether they remain stable. For this reason, we solve numerically the longitudinal GPE (7), adopting Ψ_z different from the ideal shape, i.e., equation (13). Obviously, there exists a broad range (an entire spectrum) of possible errors but, in a realistic experiment, it is reasonable to expect that it has the typical form of a bell-shaped well, similar to equation (13), and that the error will be mostly in the depth and width of such a well. Furthermore, the initial position of the BEC may be asymmetric, which leads, as we show below, to breather-like oscillations also in the parallel direction.

Our numerical results are displayed in Figure 8. They are obtained with the controlling potential in the form:

$$V_{err} = -\alpha_1 \frac{\hbar^2}{m l_z^2}\left(1 + \frac{mNl_z}{2\hbar^2} g_{1D}\right) \mathrm{sech}^2\left(\alpha_2 \frac{z - z_0}{l_z}\right). \quad (22)$$

i.e. similar to the ideal controlling potential, equation (21), but with the errors in the depth and width of the potential well, as well as in its initial position relative to the BEC. Adopting $g_{1D} = \text{const.}$, corresponding to the

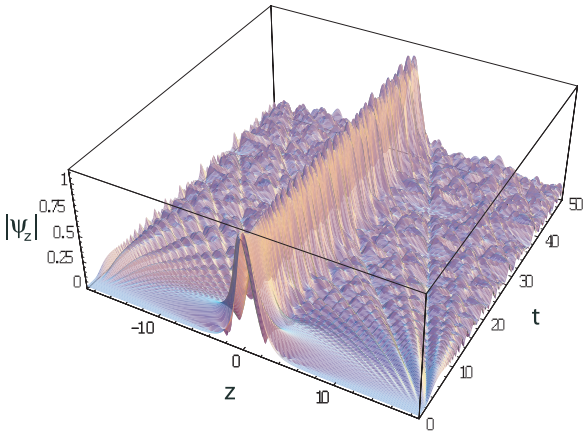

Fig. 8. The temporal evolution of $|\Psi_z(z,t)|$. The "error parameters" are adopted as $\alpha_1 = 0.9$ and $\alpha_2 = 2$, and the initial displacement of the soliton is $z_0/l_z = 0.2$. The normalizations used are $t \to t\,\hbar/2ml_z^2$, $z \to z/l_z$, and $\Psi_z \to \Psi_z/l_z$

matched case ($\sigma_{0j} = \sigma_j^*$ and $\gamma_{0j} = 0$), the "error parameters" α_1 and α_2 in the range 0.8–2.2, and the initial displacement $z_0 \sim 0.2l_z$, we obtained solutions that remained confined inside the controlling potential for a long time ($t > 100\,\hbar/g_{1D}N$) exhibiting longitudinal oscillations. Only a small part of the condensate (<10%) was lost due to "radiation", while the most part of BEC remained stable and preserved its shape. The ripples at the base of the soliton in Figure 8 are the consequence of the "radiation" that is reflected back due to the imposed period boundary conditions in the variable z, while the ruggedness of the central maximum comes from the oscillations of the soliton inside the confining potential.

5 Remarks and conclusions

We have presented a 1D stability analysis of a recently proposed method to filter and control the localized states of BEC, which seems to be possible thanks to the very recently developed techniques by controlling and manipulating the external potential well appearing in the 3D GPE. Exact controlled analytical solutions of the 3D GPE in suitable external potential wells for the ground and excited states have been found and numerically evaluated. By looking for factorized solutions, the 3D GPE is exactly decomposed into a pair of coupled equation: a transverse 2D LSE plus a 1D longitudinal GPE. It has been shown that, while the controlled BEC longitudinal profile is a bright soliton, the transverse one exhibits oscillatory breather effects. Suitable matching conditions to control this transverse BEC "respiration" have been established.

Furthermore, in the matched case ($\sigma_{j0} = \sigma_j^*$ and $\gamma_{j0} = 0$), for which the transverse BEC dynamics does not exhibit oscillations, the nonlinear coupling coefficient of the longitudinal NLSE does not depend on time. Then, the numerical integration of the longitudinal NLSE has shown breather-like oscillations of a BEC with asymmetric initial position in a confining potential that differs in shape from the ideal one. Additionally, a relatively small deviation from the ideal controlling potential will not result in destruction of the system. However, the present 1D stability analysis has been carried by perturbing the confining potential $\tilde{V}(z,t)$, which is the average (in the transverse plane) of the external potential $V_z(r_\perp, z, t)$, appearing in equation (5).

A more complete 3D stability analysis, including 3D numerical simulations, is under way and it will be considered in a future work. We expect that, in a fully 3D case, a crucial role is played by the filamentation and collapse instabilities. So, suitable conditions for the interplay between such instabilities and the controlling aspects have to be established.

References

1. L.D. Landau, E.M. Lifshitz, *Quantum Mechanics* (Pergamon Press, London, 1970)
2. L.D. Landau, E.M. Lifshitz, *Statistical Physics* (Pergamon Press, London, 1970)
3. S.N. Bose, Zeitschrift Phys. **26**, 178 (1924); A. Einstein, *Sitzungsberichte der preußischen Akademie der Wissenschaften*, 261 (1924)
4. B.P. Anderson, M.A. Kasevich, Science **282**, 1686 (1998)
5. C.J. Pethick, H. Smith, *Bose-Einstein Condensation in Diluite Gases* (Cambridge University Press, Cambridge, 2002)
6. E.A. Cornell, C.E. Wieman, Rev. Mod. Phys. **74**, 875 (2002)
7. W. Ketterle, Rev. Mod. Phys. **74**, 1131 (2002)
8. M.H. Anderson, J.R. Ensher, M.R. Matthews, C.E. Wieman, E.A. Cornell, Science **269**, 198 (1995)
9. K.B. Davis, M.-O. Mewes, M.R. Andrews, N.J. van Druten, D.S. Durfee, D.M. Kurn, W. Ketterle, Phys. Rev. Lett. **75**, 3969 (1995)
10. C.C. Bradley, C.A. Sackett, J.J. Tollett, R.G. Hulet, Phys. Rev. Lett. **75**, 1687 (1995)
11. K. Burnett, Contemporary Phys. **37**, 1 (1996)
12. A.J. Leggett, Rev. Mod. Phys. **73**, 307 (2001)
13. J. Forthàgh et al. Phys. Rev. Lett. **81**, 5310 (1998); J. Reichel, Appl. Phys. B **75**, 469 (2002); R. Folman et al., Adv. At. Mol. Opt. Phys. **48**, 263 (2002)
14. R. Grimm et al. Adv. At. Mol. Opt. Phys. **42**, 95 (2000)
15. R. Fedele, P.K. Shukla, S. De Nicola, M.A. Man'ko, V.I. Man'ko, F.S. Cataliotti, JETP Lett. **80**, 535 (2004) [Pis'ma Zh. Éksp. Teor. Fiz. **80**, 609 (2004)]; R. Fedele, P.K. Shukla, S. De Nicola, M.A. Man'ko, V.I. Man'ko, F.S. Cataliotti, Phys. Scr. **T116**, 10 (2005)
16. E.P. Gross, Nuovo Cimento **20**, 454 (1961); L.P. Pitaevskii, Sov. Phys. JETP **13**, 451 (1961)
17. F. Dalfovo et al., Rev. Mod. Phys. **71**, 463 (1999); L. Salasnich, A. Parola, L. Reatto, Phys. Rev. A **66**, 043603 (2002)
18. S. Burger et al., Phys. Rev. Lett. **83**, 15198 (1999); E.A. Donley et al., Nature **412**, 295 (2001); B.P. Anderson et al., Phys. Rev. Lett. **86**, 2926 (2001); K.E. Strecker et al., Nature **417**, 150 (2002); L. Khaykovich et al., Science **296**, 1290 (2002); B. Eiermann et al., Phys. Rev. Lett. **92**, 230401 (2004)
19. J. Lawson, *The Physics of Charged Particle Beams*, 2nd edn. (Clarendon, Oxford, 1988) and references therein
20. S. Solimeno, B. Crosignani, P. Di Porto, *Guiding, Diffraction, and Confinement of Optical Radiation* (Academic Press, Orlando, 1986) and references therein